Physics Based Electrolytic Capacitor Degradation Models for Prognostic Studies under Thermal Overstress

Chetan S. Kulkarni[1], José R. Celaya[2], Kai Goebel[3], and Gautam Biswas[4]

[1,4] *Vanderbilt University, Nashville, TN, 37235, USA*
chetan.kulkarni@vanderbilt.edu
gautam.biswas@vanderbilt.edu

[2] *SGT Inc. NASA Ames Research Center, Moffett Field, CA, 94035, USA*
jose.r.celaya@nasa.gov

[3] *NASA Ames Research Center, Moffett Field, CA, 94035, USA*
kai.goebel@nasa.gov

ABSTRACT

Electrolytic capacitors are used in several applications ranging from power supplies on safety critical avionics equipment to power drivers for electro-mechanical actuators. This makes them good candidates for prognostics and health management research. Prognostics provides a way to assess remaining useful life of components or systems based on their current state of health and their anticipated future use and operational conditions. Past experiences show that capacitors tend to degrade and fail faster under high electrical and thermal stress conditions that they are often subjected to during operations. In this work, we study the effects of accelerated aging due to thermal stress on different sets of capacitors under different conditions. Our focus is on deriving first principles degradation models for thermal stress conditions. Data collected from simultaneous experiments are used to validate the desired models. Our overall goal is to derive accurate models of capacitor degradation, and use them to predict performance changes in DC-DC converters.

1. INTRODUCTION

Most devices and systems today contain embedded electronic modules for monitoring, control and enhanced functionality. In spite of the electronic modules being used to enhance system performance and capabilities, these modules are often the first elements in the system to fail (Saha et al., 2009; Goebel et al., 2008; Saxena et al., 2008). These failures can be attributed to adverse operating conditions, such as high temperatures, voltage surges and current spikes. Studying and

analyzing the degradation of these systems (i.e.,degradation in performance) provides data that can be used to meet critical goals like advance failure warnings; (Goebel et al., 2008; Saxena et al., 2008), unscheduled maintenance;(Saha et al., 2009) which play an important role in aviation safety.

The term "diagnostics" relates to the ability to detect and isolate faults or failures in a system. "Prognostics" on the other hand is the process of predicting health condition and remaining useful life based on current state and previous conditions. Prognostics and health management (PHM) is a method that permits the assessment of the reliability of a system under its actual application conditions. PHM methods combine sensing, data collection, interpretation of environmental, operational, and performance related parameters to indicate systems health. PHM methodologies can be implemented through the use of various techniques that study parameter variations, which indicate changes in parameter degradation and operation performace based on variations in a life-cycle profile.

Prognostics and Health Management (PHM) methodologies have emerged as one of the key enablers for achieving efficient system level maintenance and safety in military systems (Saha et al., 2009). Prognostics and health management for electronic systems aims to detect, isolate, and predict the onset and source of system degradation as well as the time to system failure. The goal is to make intelligent decisions about the system health and to arrive at strategic and business case decisions. As electronics become increasingly complex, performing PHM efficiently and cost-effectively is becoming more demanding (Saha et al., 2009; J. R. Celaya et al., 2010).

In the aerospace domain, flight and ground staff need to acquire information regarding the current health state for all

subsystems of the aircraft, such as structures, propulsion, control, guidance and navigation systems on a regular basis to maintain safe operation. This has given rise to research projects that focus on accurate diagnosis of faults, developing precursors to failure, and predicting remaining component life (Balaban et al., 2010; J. R. Celaya et al., 2010). Most the avionics systems and subsystems in todays modern aircrafts contain significant electronics components which perform a critical role in on-board, autonomous functions for vehicle controls, communications, navigation and radar systems. Future aircraft systems will rely on more electric and electronic components. Therefore, this may also increase the rate of electronics related faults that occur in these systems with perhaps unanticipated fault modes that will be hard to detect and isolate. It is very important to provide system health awareness for digital electronics systems on-board, to improve aircraft reliability, assure in-flight performance, and reducing maintenance cost. An understanding of how components degrade is needed as well as the capability to anticipate failures and predict the remaining useful life of electronic components (Balaban et al., 2010; Saha et al., 2009).

1.1. Related Work

The output filter capacitor has been identified as one of the elements of a switched mode power supply that fails more frequently, and therefore, has a critical impact on performance (Vohnout et al., 2008; Goodman et al., 2007; Orsagh & et'al, 2006). A prognostics and health management (PHM) approach for power supplies of avionics systems is presented in (Orsagh & et'al, 2006).

A health management approach for multilayer ceramic capacitors is presented in the work by (Nie et al., 2007). This approach focuses on the temperature-humidity bias accelerated test to replicate failures. This approach to fault detection uses data trending algorithms in conjunction with multivariate decision-making. The Mahalanobis distance (MD) is used to detect abnormalities within the data and classify the data into "normal" and "abnormal" groups. The abnormal data are then further classified into severity levels of abnormality based on which predictions of RUL are made.

In the study done by (Gu et al., 2008), 96 multi-layer ceramic capacitors (MLCC) were selected for in-situ monitoring and life testing under elevated temperature (85°C) and humidity (85% RH) conditions with one of 3 DC voltage bias levels: rated voltage (50 V), low voltage (1.5 V), and no voltage (0 V). This method uses data from accelerated aging tests to detect potential failures and to make an estimation of time of failure. A data driven fault detection algorithm for multilayer ceramic capacitor failures is presented in (Gu & Pecht, 2008). The approach used in this study combines regression analysis, residual, detection and prediction analysis (RRDP). A method based on Mahalanobis distance is used to detect ab-

normalities in the test data; there is no prediction of RUL.

In the work done by (Wereszczak et al., 1998) the failure probability of the Barium Titanate used for the manufacturing of MLCC's was studied. Dielectric ceramics in multilayer capacitors are subjected to thermo-mechanical stresses, which, may cause mechanical failure and lead to loss of electrical function. Probabilistic life design or failure probability analysis of a ceramic component combines the strength distribution of the monolithic ceramic material comprising the component, finite element analysis of the component under the mechanical loading conditions of interest, and a multiaxial fracture criterion.

The work by (Buiatti et al., 2010) looked at the degradation in metalized polypropylene film (MPPF) capacitors, where a noninvasive technique for capacitor diagnostics in Boost converters is studied. This technique is based on the double estimations of the ESR and the capacitance, improving the diagnostic reliability and allowing for predictive maintenance using a low-cost digital signal processor (DSP).

We adopt a physics based modeling (PBM) approach to predict the dynamic behavior of the system under nominal and degraded conditions. Faults and degradations appear as parameter value changes in the model, and this provides the mechanisms for tracking system behavior under degraded conditions (Kulkarni et al., 2009).

In DC-DC power supplies used as subsytem in avionics systems (Bharadwaj et al., 2010; Kulkarni et al., 2009), electrolytic capacitors and MOSFET switches are known to have the highest degradation and failure rates among all of the components (Goodman et al., 2007; Kulkarni et al., 2009). Degraded electrolytic capacitors affect the performance and efficiency of the DC-DC converters in a significant way. We implement the PHM methodology to predict degradation in electrolytic capacitors combining the physics of failure models with data collected from experiments on the capacitors under different simulated operating conditions. In (Kulkarni, Biswas, et al., 2011b; Kulkarni, Celaya, et al., 2011) we discuss about degradation related to thermal overtress conditions and qualitative degradation mechanims. In this paper we discuss the derived physics based modeling and degradation related to thermal overstress condition (TOS) along with the experiments conducted.

2. ELECTROLYTIC CAPACITORS

Electrolytic capacitor performance is strongly affected by its operating conditions, such as voltage, current, frequency, and ambient temperatures. When capacitors are used in power supplies and signal filters, degradation in the capacitors increases the impedance path for the AC current and decrease in capacitance introduces ripple voltage on top of the desired DC voltage. Continued degradation of the capacitor leads the

converter output voltage to drop below specifications affecting downstream components. In some cases, the combined effects of the voltage drop and the ripples may damage the converter and downstream components leading to cascading failures in systems and subsystems.

A primary reason for wear out in aluminum electrolytic capacitors is due to vaporization of electrolyte (Goodman et al., 2007) and degradation of electrolyte due to ion exchange during charging/discharging (Gomez-Aleixandre et al., 1986; Ikonopisov, 1977), which, in turn leads to a drift in the two main electrical parameters of the capacitor: (1) the equivalent series resistance (ESR), and (2) the capacitance (C). The ESR of a capacitor is the sum of the resistance due to aluminum oxide, electrolyte, spacer, and electrodes (foil, tabbing, leads, and ohmic contacts) (Hayatee, 1975; Gasperi, 1996). The health of a capacitor is often indicated by the values of these two parameters. There are certain industry standard thresholds for these parameter values, upon crossing these threshold barrier the component is considered unhealthy to be used in a system, i.e., the component has reached its end of life, and should be immediately replaced before further operations (Lahyani et al., 1998; Eliasson, 2007; Imam et al., 2005).

As illustrated in Fig. 1 an aluminum electrolytic capacitor, consists of a cathode aluminum foil, electrolytic paper, electrolyte, and an aluminum oxide layer on the anode foil surface, which acts as the dielectric. When in contact with the electrolyte, the oxide layer possesses an excellent forward direction insulation property (Gasperi, 1996). Together with magnified effective surface area attained by etching the foil, a high capacitance value is obtained in a small volume (Fife, 2006). Since the oxide layer has rectifying properties, a ca-
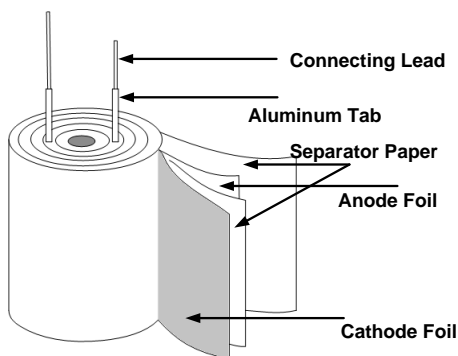

Figure 1. Physical Model of Electrolytic Capacitor

pacitor has polarity. If both the anode and cathode foils have an oxide layer, the capacitors would be bipolar. In this work, we analyze "non-solid" aluminum electrolytic capacitors in which the electrolytic paper is impregnated with liquid electrolyte. The another type of aluminum electrolytic capacitor, that uses solid electrolyte (Bengt, 1995) is not discussed in this work.

2.1. Overview of Degradation Mechanisms

The flow of current during the charge/ discharge cycle of the capacitor causes the internal temperature to rise. The heat generated is transmitted from the core to the surface of the capacitor body, but not all the heat generated can escape. The excess heat results in a rise in the internal temperature of the capacitors which causes the electrolyte to evaporate, and gradually deplete (Kulkarni, Biswas, et al., 2011b; Kulkarni, Celaya, et al., 2011). Similarly in situations where the capacitor is operating under high temperature conditions, the capacitor body is at a higher temperature than its core, the heat travels in the opposite directions from the body surface to the core of the capacitor again increasing the internal temperature causing the electrolyte to evaporate. This is explained using a first principles thermal model of heat conduction (Kulkarni, Biswas, et al., 2011b; Kulkarni, Celaya, et al., 2011).

Degradation in the oxide layer can be attributed to crystal defects that occur because of the periodic heating and cooling during the capacitor's duty cycle, as well as stress, cracks, and installation-related damage. High electrical stress is known to accentuate the degradation of the oxide layer due to localized dielectric breakdowns on the oxide layer (Ikonopisov, 1977; Wit & Crevecoeur, 1974). These breakdowns, which accelerate the degradation, have been attributed to the duty cycle, i.e., the charge/discharge cycle during operation (Ikonopisov, 1977). Further another simultaneous phenomenon is the increase in the internal pressure (Gomez-Aleixandre et al., 1986) due to an increased rate of chemical reactions, which can again be attributed to the internal temperature increase in the capacitor. This pressure increase can ultimately lead to the capacitor popping.

All the failure/degradation phenomenon mentioned may act simultaneously based on the operating conditions of the capacitors. We first study the phenomenon qualitatively, and then discuss the steps to derive the first principles analytic degradation models for the different thermal stress condition. Electrolyte evaporations is caused either due to increase in internal core temperature or external surrounding temperature. Both phenomenon lead to the same degradation mode, caused either by the high electrical stress or thermal stress, respectively.

3. THERMAL OVERSTRESS EXPERIMENT

In this setup we emulated conditions similar to high temperature storage conditions (Kulkarni, Biswas, et al., 2011b; Kulkarni, Celaya, et al., 2011), where capacitors are placed in a controlled chamber and the temperature is raised above their rated specification (60068-1, 1988). Pristine capacitors were taken from the same lot rated for 10V and maximum storage temperature of 85°C.

The chamber temperature was gradually increased in steps of 25°C till the pre-determined temperature limit was reached. The capacitors were allowed to settle at a set temperature for 15 min and then the next step increase was applied. This process was continued till the required temperature limit was attained. To decrease possibility of shocks due to sudden decrease in the temperature the above procedure was followed.

Experiments done with 2200 μF capacitors with TOS temperature at 105°C and humidity factor at 3.4%. At the end of specific time interval the temperature was lowered in steps of 25°C till the required room temperature was reached. Before being characterized the capacitors were kept at room temperature for 15 min. The ESR value is the real impedance measured through the terminal software of the instrument. Similarly the capacitance value is computed from the imaginary impedance using Electrochemical Impedance Spectroscopy (EIS). Characterization of all the capacitors was done for measuring the impedance values using an SP-150 Biologic impedance measurement instrument (Biologic, 2010).
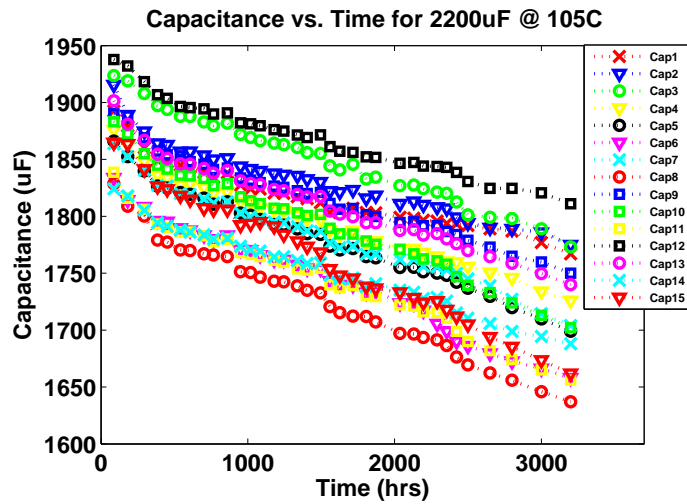

Figure 2. Capacitance Plot for all the devices under TOS

4. PHYSICS BASED MODELING OF CAPACITOR DEGRADATION

Based on the above discussions on degradation and experiments conducted, in this section we discuss about deriving the first principles models for thermal overstress conditions. Under thermal overstress conditions since the device was subjected to only high temperature with no charge applied we observe degradation only due to electrolyte evaporation. The models are derived based on this observations and measurements see during from the experimental data.

For deriving the physics based models it is also very much necessary to know about the structural details of the component under study. The models defined use this information

for making effective degradation/failure predictions. A detail structural study of the electrolytic capacitor under test is discussed in this section.

During modeling it is not possible to know the exact amount of electrolyte present in a capacitor. But using information from the structure details we can approximately calculate the amount of electrolyte present. Based on the type and configuration, the electrolyte volume will vary which can be updated in the model parameters. The equation for calculating the approximate electrolyte volume is derived from calculating the volume of the total capacitor capsule, is given by :

$$V_c = \pi r_c^2 h_c \tag{1}$$

The amount of electrolyte present depends on the type of paper used as a separator between the anode and cathode foils. A highly porous paper type is used in the construction of the capacitor such that maximum amount of electrolyte can be soaked in the paper. The electrolyte is completely soaked in the paper spacer. Hence the electrolyte volume can be approximated as :

$$V_e \approx V_{paper} \tag{2}$$

The approximate volume of electrolyte, V_e based on geometry of the capacitor is expressed in terms of following equation:

$$V_e = \pi r_c^2 h_c - A_{surface}(d_A + d_C) \tag{3}$$

A simplified electrical lumped parameter model of impedance, $\mathcal{M}_1$ defined for a electrolytic capacitor is as shown in Fig.3. The ESR dissipates some of the stored energy in the capacitor. In spite of the dielectric insulation layer between a capacitor's plates, a small amount of 'leakage' current flows between the plates. For a good capacitor operating nominally this current is not significant, but it becomes larger as the oxide layer degrades during operation. An ideal capacitor would offer no resistance to the flow of current at its leads. However, the electrolyte , aluminum oxide , space between the plates and the electrodes combined produces a small equivalent internal series resistance.
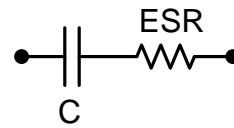

Figure 3. Lumped Parameter Model ($\mathcal{M}_1$)

From the literature (Rusdi et al., 2005; Bengt, 1995; Roederstein, 2007) and experiments conducted under thermal overstress, it has been observed that the capacitance and ESR value depends of the electrolyte resistance R_E. A more detailed lumped parameter model derived for an electrolytic capacitor under thermal overstress condition, $\mathcal{M}_2$ can be modified from $\mathcal{M}_1$, as shown in Fig. 4. R_1 is the combined series

and parallel resistances in the model. R_E is the electrolyte resistance. The combined resistance of R_1 and R_E is the equivalent series resistance of the capacitor. C is the total capacitance of the capacitor as discussed earlier.
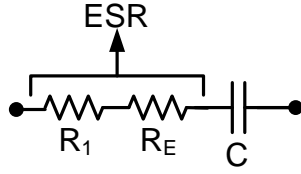

Figure 4. Updated Lumped Parameter Model ($\mathcal{M}_2$)

4.1. First Principle Models

The input impedance of the capacitor network is defined in terms of the total lumped series and parallel impedance of the simplified network. The total lumped capacitance of the structure is given by

$$C = (2\epsilon_R \epsilon_0 A_{surface})/d_C \qquad (4)$$

From the literature study (Rusdi et al., 2005; Bengt, 1995) for modeling ESR degradation it was observed that electrolyte resistance (R_E) parameter, as discussed above forms a major part of combined ESR as shown in Fig. 3. Thus being a dominant parameter any changes in R_E lead to changes in the ESR value. We studied the relationship between R_E and $A_{surface}$, which gives us a degradation model for ESR. The equation for R_E is given by :

$$R_E = \rho_E \, d_C \, P_E/(2 * L * H) \qquad (5)$$

Since R_E is a dominant parameter in ESR and any changes in R_E affect ESR value, from Eq. (5) we express ESR in terms of the oxide surface area, $A_{surface}$ as:

$$ESR = \rho_E \, d_C \, P_E/(2 * A_{surface}) \qquad (6)$$

Exposure of the capacitors to temperatures $T_{applied} > T_{rated}$ results in accelerated aging of the devices (Kulkarni, Celaya, et al., 2011; Kulkarni, Biswas, et al., 2011a; 60068-1, 1988). Higher ambient storage temperature accelerates the rate of electrolyte evaporation leading to degradation of the capacitance (Kulkarni, Celaya, et al., 2011; Bengt, 1995). The depletion in the volume and thus the effective surface area is given by Eq. (7).

$$V = V_o - (A_{surface} \, j_{eo} \, w_e) \times t \qquad (7)$$

Details of the derivation of this equation can be found in (Kulkarni, Biswas, et al., 2011b; Rusdi et al., 2005). Evaporation also leads to increase in the internal pressure of the capacitor, which decreases electrolyte evaporation rate. Eq. (9) and Eq. (8) give us the decrease in the active surface area due to evaporation of the electrolyte, which results in a decrease in C and an increase in ESR, respectively (Bengt, 1995; Roederstein, 2007).

4.1.1. Capacitance Degradation Model

Thus from Eq. (4) and (7) we can derive the first principles capacitance degradation model, $\mathcal{D}_1$ which is given by :

$$\mathcal{D}_1 : C(t) = \left[\frac{2\epsilon_R \epsilon_0}{d_C}\right] \left[\frac{V_0 - V(t)}{j_{eo} \, t \, w_e}\right] \qquad (8)$$

The degradation in capacitance is directly proportional to the damage parameter V. As discussed earlier, increase in the core temperature evaporates the electrolyte thus decreasing the electrolyte volume leading to degradation in capacitance. The resultant decrease in the capacitance can be computed using Eq. (8).

4.1.2. ESR Degradation Model

From Eq. (6) and Eq. (7) the ESR degradation model, $\mathcal{D}_2$ is given as :

$$\mathcal{D}_2 : ESR(t) = \left[\frac{\rho_E \, d_C \, P_E}{2}\right] \left[\frac{j_{eo} \, w_e \, t}{V_0 - V(t)}\right] \qquad (9)$$

In this model there are two parameters which change with time, rate of evaporation j_{eo} and the correlation factor related to electrolyte spacer porosity and average liquid pathway, P_E. As the electrolyte evaporates due to high temperature the correlation factor P_E will increase as the average pathway of the liquid decreases. Electrolyte evaporation under thermal stress storage condition results due to the increase in the high atmospheric temperature. Under this operating condition when the surrounding temperature gets high, the temperature of the capacitor capsule also increases. Heat travels from the surface of the body to the core of the temperature, this phenomenon is described through the thermal model (Kulkarni et al., 2009; Kulkarni, Celaya, et al., 2011).

The decrease in the capacitance parameter value is as a result of the decrease in electrolyte volume due to evaporation under thermal overstress condition. This relationship between decrease in capacitance with electrolyte volume is explained by Eq. (8). Similarly increase in ESR is given by the increase in the electrolyte resistance (R_E) as explained by Eq. (9). With decrease in the electrolyte due to thermal overstress, the average liquid path length is reduced, which increases P_E. Under normal circumstances when the capacitors are stored at room temperature or below rated temperatures, no damage or decrease in the life expectancy is observed. But in cases where the capacitors are stored under thermal stress conditions permanent damage is observed.

In the thermal overstress experiments, the capacitors we characterized periodically and after 3400 hours of operation it was observed that the average capacitance (C) value decreased by more than 8-9% while increase in the ESR value was observed around 20 - 22%. From literature (60068-1, 1988)

under thermal overstress conditons higher capaitance degradation is observed and minor degradation in ESR which correlated with the data collected. The failure thresholds under storage conditions for capacitance (C) is 10% while that for ESR is around 280- 300% of the pristene condition values (60384-4-1, 2007; Kulkarni, Biswas, et al., 2011b). Based on the degradation observed from the experiments capacitance degradation was considered as a precursor to failure to estimate the current health condition of the device.

5. DEGRADATION MODELING

In our earlier work (J. Celaya et al., 2011b, 2011a; Kulkarni et al., 2012) an implementation of a model-based prognostics algorithm based on Kalman filter and a physics inspired empirical degradation model has been presented. The physics inspired degradation model was derived based on the capacitance degradation data from electrical overstress experiments. This model relates aging time to the percentage loss in capacitance and has the following form,

$$C(t) = e^{\alpha t} + \beta, \qquad (10)$$

where model constants α and β were estimated from the experimental data. Here the exponential model was linked to the degradation data and parameters were derived based on this data. The exponential empirical model derived in Eq. (10) was further updated and as discussed in section (4.1.1) we developed a first principles based generalized model to be implemented for different capacitor types and operating conditions. In this work we looked into the degradation data under thermal overstress as discussed earlier and use Eq.(8) to build the physics based model based on following equation:

Here in this section we will discuss the parameter estimation work done and study how well the developed degradation model, $\mathcal{D}_1$ behaves based on the estimated static parameters. As an initial step we implement a nonlinear least-squares regression algorithm to estimate the model parameters.
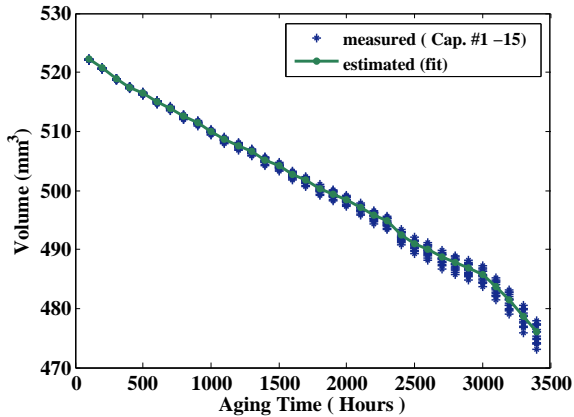
Figure 5. Estimation results for Volume decrease

Decrease in capacitance parameter is used as a precursor of failure. Based on the experiments, capacitance parameter values are computed by characterizing the capacitors as shown in plots of Fig. 2. From the degradation model, $\mathcal{D}_1$ given a certain type of capacitor all the values in Eq. (8) can be computed except the dispersion volume V. Therefore dispersion volume V is computed based on the available data and used to build a physics based model, $\mathcal{D}_1$ of the degradation phenomenon. Initial electrolyte volume V_o at pristine conditions is approximately computed from the physics and geometry of the capacitor. From the experimental data the estimated volume computed decreases almost linearly through the initial phase of degradation. Hence in this work we propose a linear dynamic model, which relates aging time to loss of electrolyte volume. The loss in electrolyte is linked to decrease in capacitance through Eq. (8) and has the following form,

$$V_k = \hat{\theta}_1 + \hat{\theta}_2\, t_k + \hat{\theta}_3\, {t_k}^2 \qquad (11)$$

where $\hat{\theta}_1$, $\hat{\theta}_2$ and $\hat{\theta}_3$ are model constants for decrease in volume V, which is estimated from the experimental data of accelerated thermal aging experiments. In order to estimate the model parameters, 14 capacitors out of the 15 were used for the experiment, (labeled capacitors #1 through #15), and the remaining capacitor is used to validate the model against experimental data. A nonlinear least-squares regression algorithm is used to estimate the model parameters.
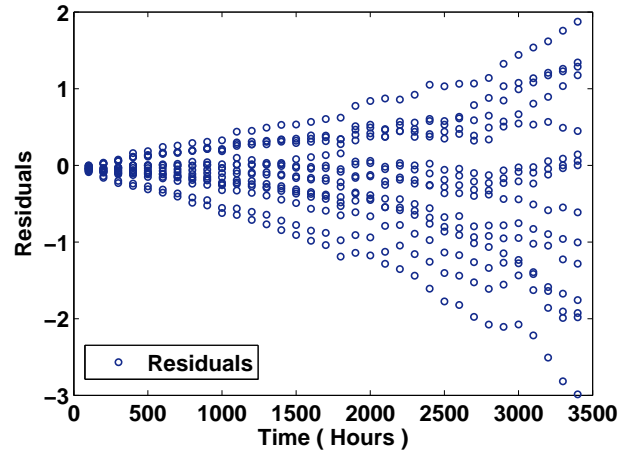
Figure 6. Residuals

The experimental data is presented together with results from the linear fit function of Eq. (11) and Eq. (8), as shown in Fig. 5. It can be observed from the residuals of Fig. 6 that the estimation error increases with time. This is to be expected since the data takes a concave path after approximately 2500 hours of operation, a dip is observed in the linear degradation and hence we observe higher residuals values. This indicates that the phenomenon of volume decrease is not linear and we are working towards updating the model in Eq. (11). The updated model will include additional degradation phenomenons in addition to the current model explained which

will take into consideration the dipping in the volume parameter during the later stages of aging as observed.
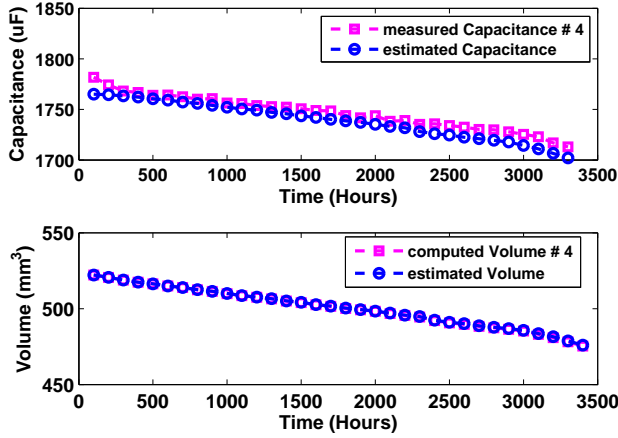

Figure 7. Volume and Capacitance Estimation (Cap # 4)

The updated degradation model is used as part to estimate the capacitance based on the estimated decrease in volume. In Fig.7, based on the data from capacitors other than capacitor #4, volume parameters were estimated. This was validated against the change in volume of capacitor #4, and the model, $\mathcal{D}_1$ was validated for decrease in capacitance.

Case	$\hat{\theta}_1$	$\hat{\theta}_2$	$\hat{\theta}_3$	MSE
1	523.6123	-0.01613	$3.7100*10^{-7}$	685.6593
2	523.6122	-0.01613	$3.7099*10^{-7}$	685.0815
3	523.6159	-0.01614	$3.9403*10^{-7}$	684.3579
4	523.6109	-0.01609	$3.8072*10^{-7}$	687.3755
5	523.6128	-0.01614	$3.8428*10^{-7}$	688.3824
6	523.6100	-0.01613	$3.7867*10^{-7}$	690.6146
7	523.6081	-0.01614	$3.7269*10^{-7}$	688.1003
8	523.6089	-0.01613	$3.7988*10^{-7}$	691.7173
9	523.6111	-0.01616	$3.7447*10^{-7}$	686.0799
10	523.6122	-0.01613	$3.8470*10^{-7}$	687.8928
11	523.6076	-0.01611	$3.7350*10^{-7}$	690.5650
12	523.6065	-0.01614	$3.7313*10^{-7}$	683.0697
13	523.6147	-0.01609	$3.8906*10^{-7}$	686.4739
14	523.6120	-0.01612	$3.8276*10^{-7}$	689.6318
15	523.6113	-0.01616	$3.8317*10^{-7}$	689.8948
$\bar{X}$	523.6112	-0.0161	$3.8077*10^{-7}$	687.6598
$\tilde{X}$	523.6113	-0.0161	$3.8072*10^{-7}$	687.8928
S.D	0.0026	$1.8748*10^{-5}$	$6.9373*10^{-9}$	2.5339
C.I	523.6098	-0.01614	$0.3769*10^{-6}$	686.2565
	523.6127	-0.01611	$0.3846*10^{-6}$	689.0630

Table 1. Parameter Estimation Results

Table 1 shows the estimated values of the parameters for each capacitor along with the mean square error observed for the estimated values.

6. CONCLUSION AND DISCUSSION

This paper presents a first principles based degradation electrolytic capacitor model and a parameter estimation algorithm to validate the derived model, based on the experimental data. The major contributions of the work presented in this paper are:

1. Identification of the lumped-parameter model, $\mathcal{M}_1$ and $\mathcal{M}_2$ (Fig. 3 and Fig. 4) based on the equivalent electrical circuit of a real capacitor as a viable reduced-order model for prognostics-algorithm development;

2. Identification of capacitance (C) as a failure precursor in the lumped parameter model, $\mathcal{M}_1$ as shown in Fig. 3;

3. Estimating the electrolyte volume from structural model of the capacitor to be implemented in the first principles degradation model, $\mathcal{D}_1$;

4. Development of the first principles degradation model based on accelerated life test aging data which includes decrease in capacitance as a function of time and evaporation rate linked to temperature conditions;

5. Implementation of parameter estimation algorithm to cross validate the derived first principles degradation model, $\mathcal{D}_1$.

The degradation model, $\mathcal{D}_1$ based on the first principles gives an indication of how a specific device degrades based on its geometrical structure, operating conditions, etc. The derived model can be updated and developed at a more finer granular level to be implemented for detailed prognostic implementation. The results presented here are based on accelerated aging experimental data and on the accelerated life timescale. In our earlier work physics inspired degradation models based on the observed data were discussed (J. Celaya et al., 2011b, 2011a). The work discussed in this paper is a next step to generalize the degradation model and has been tested for the current data of capacitors under constant temperature of 105°C. As discussed in section (5), as a first step an linear model has been implemented for decrease in volume, V and needs to be updated to include the operating condition variables.

The performance of the proposed first principles degradation model, $\mathcal{D}_1$ is satisfactory for this study based on the quality of the model fit to the experimental data and cross validation performance based on the parameter estimations done. In this work, our major emphasis was on deriving the first principles model for degradation and validating the model with a basic non-linear regression model. Our future work will focus on exploring a detailed implementation of the physics based model to Bayesian approach which can then be used for making more accurate degradation and failure predictions. The other focus point will be on using the physics based model to validate the capacitor data under different thermal conditions and capacitor geometry. This will greatly enhance the qual-

ity and effectiveness of the degradation models in prognostics, where the operating and environmental conditions along with the structural conditions are also accounted for towards degradation dynamics.

NOMENCLATURE

ϵ_R	relative dielectric constant
ϵ_O	permitivity of free space
t_o	oxide thickness
V	dispersion volume at time t
V_O	initial electrolyte volume
j_{eo}	evaporation rate (mg min^{-1} $area^{-1}$)
t	time in minutes
ρ_E	electrolyte resistivity
P_E	correlation factor related to electrolyte spacer porosity and average liquid pathway.
r_c	radius of capacitor capsule
h_c	height of capacitor capsule
V_{paper}	volume of paper.
L	length of the anode oxide surface
H	height of the anode oxide surface
$A_{surface}$	effective oxide surface area (L x H)
w_e	volume of ethyl glycol molecule
V_c	total capacitor capsule volume
d_A	thickness of anode strip,
d_C	thickness of cathode strip
C	capacitance
$\mathcal{M}_1$	electrical lumped parameter model
$\mathcal{M}_2$	updated lumped parameter model
$\mathcal{D}_1$	capacitance degradation model
$\mathcal{D}_2$	ESR degradation model

REFERENCES

60068-1, I. (1988). Environmental testing, Part 1: General and guidance. *IEC Standards*.

60384-4-1, I. (2007). Fixed capacitors for use in electronic equipment. *IEC Standards*.

Balaban, E., Saxena, A., Narasimhan, S., Roychoudhury, I., Goebel, K., & Koopmans, M. (2010). Airborne Electro-Mechanical Actuator Test Stand for Development of Prognostic Health Management Systems. *Proceedings of Annual Conference of the PHM Society 2010, October 10-16, Portland, OR*.

Bengt, A. (1995). Electrolytic Capacitors Theory and Applications. *RIFA Electrolytic Capacitors*.

Bharadwaj, R., Kulkarni, C., Biswas, G., & Kim, K. (2010, April). Model-Based Avionics Systems Fault Simulation and Detection. *American Institute of Aeronautics and Astronautics, AIAA Infotech@Aerospace 2010, AIAA-2010-3328*.

Biologic. (2010). Application note 14-Zfit and equivalent electrical circuits [Computer software manual].

Buiatti, G., Martin-Ramos, J., Garcia, C., Amaral, A., & Cardoso, A. (2010). An Online and Noninvasive Technique for the Condition Monitoring of Capacitors in Boost Converters. *IEEE Transactions on Instrumentation and Measurement*, 59, 2134 - 2143.

Celaya, J., Kulkarni, C., Biswas, G., & Goebel, K. (2011a). A Model-based Prognostics Methodology for Electrolytic Capacitors Based on Electrical Overstress Accelerated Aging. *Proceedings of Annual Conference of the PHM Society, September 25-29, Montreal, Canada*.

Celaya, J., Kulkarni, C., Biswas, G., & Goebel, K. (2011b). Towards Prognostic of Electrolytic Capacitors. *American Institute of Aeronautics and Astronautics, AIAA Infotech@Aerospace 2011, March 2011, St. Louis, Missouri*.

Celaya, J. R., Wysocki, P., Vashchenko, V., Saha, S., & Goebel, K. (2010). Accelerated aging system for prognostics of power semiconductor devices. In *IEEE AUTOTESTCON, 2010* (p. 1-6). Orlando, FL.

Eliasson, L. (2007, October - November). Aluminium Electrolytic Capacitor's performance in Very High Ripple Current and Temperature Applications. *CARTS Europe 2007 Symposium, Spain*.

Fife, J. (2006, Aug). *Wet Electrolytic Capacitors* (Patent No: 7,099 No. 1). Myrtle Beach, SC: AVX Corporation.

Gasperi, M. L. (1996, October). Life Prediction Model for Aluminum Electrolytic Capacitors. *31st Annual Meeting of the IEEE-IAS*, 4(1), 1347-1351.

Goebel, K., Saha, B., & Saxena, A. (2008). A Comparision of Three Data-Driven Tes for Prognostics. *62nd Meeting of the Society For Machinery Failure Prevention Technology (MFPT) Virginia Beach, VA*, 119 - 131.

Gomez-Aleixandre, C., Albella, J. M., & Martnez-duart, J. M. (1986). Pressure build-up in aluminum electrolytic capacitors under stressed voltage conditions. *Journal of Applied Electrochemistry*, *Volume 16, Number 1*, 109 - 115.

Goodman, D., Hofmeister, J., & Judkins, J. (2007). Electronic prognostics for switched mode power supplies. *Microelectronics Reliability*, *47(12)*, 1902-1906.

Gu, J., Azarian, M. H., & Pecht, M. G. (2008). Failure Prognostics of Multilayer Ceramic Capacitors in Temperature-Humidity-Bias Conditions. *International Conference on Prognostics and Health Management*.

Gu, J., & Pecht, M. (2008). Prognostics and Health Management Using Physics-of-Failure. *54th Annual Reliability and Maintainability Symposium (RAMS)*.

Hayatee, F. G. (1975). Heat Dissipation and Ripple Current rating in Electrolytic Capacitors. *Electrocomponent Science and Technology*, 2, 109-114.

Ikonopisov, S. (1977). Theory of electrical breakdown during formation of barrier anodic films. *Electrochimica Acta*, *,Volume 22, Issue 10*, 1077 - 1082.

Imam, A., Habetler, T., Harley, R., & Divan, D. (2005, June). Condition Monitoring of Electrolytic Capaci-

tor in Power Electronic Circuits using Adaptive Filter Modeling. *IEEE 36th Power Electronics Specialists Conference, 2005. PESC '05.*, 601-607.

Kulkarni, C., Biswas, G., Celaya, J., & Goebel, K. (2011a). A Case Study for Capacitor Prognostics under Accelerated Degradation. *IEEE 2011 Workshop on Accelerated Stress Testing & Reliability (ASTR), September 28-30, San Francisco, CA.*

Kulkarni, C., Biswas, G., Celaya, J., & Goebel, K. (2011b). Prognostic Techniques for Capacitor Degradation and Health Monitoring. *The Maintenance& Reliability Conference, MARCON 2011, Knoxville, TN*.

Kulkarni, C., Biswas, G., & Koutsoukos, X. (2009). A prognosis case study for electrolytic capacitor degradation in DC-DC converters. *Proceedings of Annual Conference of the PHM Society, September 27 October 1, San Diego, CA*.

Kulkarni, C., Celaya, J., Biswas, G., & Goebel, K. (2011). Prognostic Modeling and Experimental Techniques for Electrolytic Capacitor Health Monitoring. *The 8th International Workshop on Structural Health Monitoring 2011 (IWSHM), September 13-15, Stanford University, Stanford, CA*.

Kulkarni, C., Celaya, J., Biswas, G., & Goebel, K. (2012). Prognostic and Experimental Techniques for Electrolytic Capacitor Health Monitoring. *The Annual Reliability and Maintainability Symposium (RAMS), January 23-36, Reno, Nevada.*.

Lahyani, A., Venet, P., Grellet, G., & Viverge, P. (1998, Nov). Failure prediction of electrolytic capacitors during operation of a switchmode power supply. *IEEE Transactions on Power Electronics*, 13, 1199-1207.

Nie, L., Azarian, M., Keimasi, M., & Pecht, M. (2007). Prognostics of ceramic capacitor temperature humidity bias reliability using mahalanobis distance. *Circuit World*, 33(3), 21 - 28.

Orsagh, R., & et'al. (2006, March). Prognostic Health Management for Avionics System Power Supplies. *Aerospace Conference, 2006 IEEE*, 1-7.

Roederstein, V. (2007). Aluminum Capacitors - General Information. *Document - 25001 January 2007*.

Rusdi, M., Moroi, Y., Nakahara, H., & Shibata, O. (2005). Evaporation from Water Ethylene Glycol Liquid Mixture. *Langmuir - American Chemical Society*, 21 (16), 7308 - 7310.

Saha, B., Celaya, J. R., Wysocki, P. F., & Goebel, K. F. (2009). Towards prognostics for electronics components. In *IEEE Aerospace conference 2009* (p. 1-7). Big Sky, MT.

Saxena, A., Celaya, J., Balaban, E., Goebel, K., Saha, B., Saha, S., et al. (2008). Metrics for evaluating performance of prognostic techniques. In *International Conference on Prognostics and Health Management 2008.*

Vohnout, S., Kozak, M., Goodman, D., Harris, K., & Judkins, J. (2008). Electronic Prognostics System Implementation on Power Actuator Components. *Aerospace Conference, 2008 IEEE*, 1 - 11.

Wereszczak, A., Breder, K., & Ferber, M. K. (1998). Failure Probability Prediction of Dielectric Ceramics in Multilayer Capacitors. *Annual Meeting of the American Ceramic Society, Cincinnati, OH (United States)*.

Wit, H. D., & Crevecoeur, C. (1974). The dielectric breakdown of anodic aluminum oxide. *Physics Letters A*, *Volume 50, Issue 5*, 365 - 366.

Chetan S. Kulkarni is a Research Assistant at ISIS, Vanderbilt University. He received the M.S. degree in EECS from Vanderbilt University, Nashville, TN, in 2009, where he is currently a Ph.D candidate and received a B. E. degree in Electronics and Electrical Engineering from University of Pune, India in 2002.

José R. Celaya is a research scientist with SGT Inc. at the Prognostics Center of Excellence, NASA Ames Research Center. He received a Ph.D. degree in Decision Sciences and Engineering Systems in 2008, a M. E. degree in Operations Research and Statistics in 2008, a M. S. degree in Electrical Engineering in 2003, all from Rensselaer Polytechnic Institute, Troy New York; and a B. S. in Cybernetics Engineering in 2001 from CETYS University, México.

Kai Goebel received the degree of Diplom-Ingenieur from the Technische Universitt Mnchen, Germany in 1990. He received the M.S. and Ph.D. from the University of California at Berkeley in 1993 and 1996, respectively. Dr. Goebel is a senior scientist at NASA Ames Research Center where he leads the Diagnostics and Prognostics groups in the Intelligent Systems division. In addition, he directs the Prognostics Center of Excellence and he is the technical lead for Prognostics and Decision Making of NASAs System-wide Safety and Assurance Technologies Program. He worked at General Electrics Corporate Research Center in Niskayuna, NY from 1997 to 2006 as a senior research scientist. He has carried out applied research in the areas of artificial intelligence, soft computing, and information fusion. His research interest lies in advancing these techniques for real time monitoring, diagnostics, and prognostics. He holds 15 patents and has published more than 200 papers in the area of systems health management.

Gautam Biswas received the Ph.D. degree in computer science from Michigan State University, East Lansing. He is a Professor of Computer Science and Computer Engineering in the Department of Electrical Engineering and Computer Science, Vanderbilt University, Nashville, TN.